Available online at www.sciencedirect.com
ScienceDirect
Acta Materialia 55 (2007) 5684–5696
Acta MATERIALIA
www.elsevier.com/locate/actamat

Quantitative evaluation of fracture, healing and re-healing of a reversibly cross-linked polymer

Thomas A. Plaisted [1], Sia Nemat-Nasser *

Center of Excellence for Advanced Materials, Department of Mechanical and Aerospace Engineering, University of California, San Diego, CA 92093-0416, USA

Received 17 January 2007; received in revised form 1 June 2007; accepted 5 June 2007
Available online 4 September 2007

Abstract

The repeated fracture–healing characteristics of 2MEP4F polymer, a cross-linked polymer based on Diels–Alder cycloaddition, are systematically and quantitatively evaluated using a sample geometry that allows for controlled incremental crack growth so that the cracked sample remains in one piece after the test, improving our ability to realign the fracture surfaces prior to healing. The specimens have been pre-cracked to a repeatable length to enable accurate comparison between virgin and healed fracture loads, and hence fracture toughness. Moreover, multiple data points are extracted from a single sample. In this paper, we report the results of our repeated fracturing and healing cycles. We have shown that healing at temperatures between 85 and 95 °C, after repeated fracture–healing cycles, results in full fracture toughness recovery and no dimensional changes due to creep. We have then calculated the fracture toughness after each fracturing and healing cycle, using a previously developed and tested model, arriving at consistent results for repeatedly healed 2MEP4F polymer. These results show a fracture toughness of about 0.71 MPa $m^{1/2}$ for this material at room temperature. We have also examined healing for shorter periods, as little as 30 min, using the same temperature–pressure cycle, arriving at essentially the same final results, i.e., full toughness recovery. That the healing process is largely independent of time is in contrast to the diffusion-controlled healing observed in the welding of thermoplastic polymers. Rather, it shows that the healing in the 2MEP4F polymer results from the repair of the broken Diels–Alder (cross-linking) bonds that seems to restore a molecular structure similar to that of the original virgin polymer with the same (or even slightly improved) overall macroscopic fracture resistance.

Keywords: Healable polymers; Fracture toughness; Repeated fracture–healing

1. Introduction

A material that can heal itself is of great utility where access for manual repair is limited or impossible, as in a biological implant or a material that is launched into orbit in outer space. Structures made of such materials may have significantly prolonged service life in addition to improved safety if failure in the form of cracking can be repaired in situ. Nature has long demonstrated this property in various biological materials, whereas, until recently, man-made healable materials have essentially not been demonstrated. Recently, interest in synthetic healable materials has gained some attention with the creation of an autonomic healable polymer by White et al. [2]. In this system, microencapsulated liquid monomer is embedded with dispersed catalyst in a thermoset polymer, such that a propagating crack which intersects and fractures the microcapsules causes a release of the healing agent to fill the crack opening region. An alternate approach to healing is to develop a polymer with the ability to repair internal cracks by using a thermally reversible Diels–Alder (DA) and retro-DA cycloaddition. Many polymers involving the DA cycloaddition have been synthesized, though in many cases the retro-DA reaction is not observed if the

* Corresponding author.
E-mail address: sia@ucsd.edu (S. Nemat-Nasser).
[1] Present address: Luna Innovations Inc., Blacksburg, VA 24060, USA.

1359-6454/$30.00
doi:10.1016/j.actamat.2007.06.019

diene and dieneophile are not sufficiently stable on their own. Those polymers with suitable monomer combinations to exhibit the retro-DA reaction have incorporated the DA adduct into the backbone of the polymer [3–5]. Recently, Chen et al. [6,7] have succeeded in creating healable polymers such that all of the monomer linkages, or cross-links, are formed by DA cycloaddition and furthermore, by careful design of the monomers, exhibit the retro-DA reaction.

The repair mechanism of these polymers relies on a DA bond, as illustrated in Fig. 1 for 2MEP4F polymer. This covalent bond is weaker than other bonds in the polymer backbone, so that, when the sample is loaded excessively, it will break preferentially along these bonds as compared with the other covalent bonds in the molecule. Chen et al. previously reported the bond energy of the DA adduct to be about 23 kcal mol^{-1} by measuring the exotherm during polymerization of similar maleimide and furan monomers [7]. Above ~110 °C, the bonds will also disconnect (retro-DA cycloaddition), such that approximately 12% disconnect after 25 min at 130 °C for 3M4F polymer [6]. Below 110 °C, the stable state of the DA moieties is to re-connect as a cycloadduct. Thus, healing is achieved by bringing the broken DA moieties into proximity of one another at a temperature below 110 °C. This suggests that macrocracks in the polymer can be healed by bringing the fractured interfaces together through pressure at suitable temperatures to accelerate healing while avoiding creep, and then cooling the polymer to room temperature. Heating provides sufficient conformational motion in the polymer structure to bring the de-bonded maleimide and furan groups into close proximity. In theory, the bond will self-repair at any temperature below the retro-DA temperature (110 °C) provided that the broken moieties come into contact.

Repair of a significant fraction of the broken cross-links should lead to a commensurate recovery of the polymer's macroscopic fracture strength (e.g., the energy-release rate, or equivalently, the fracture toughness). The macroscopic toughness of the polymer stems from the energy loss due to various micro- and macromechanisms that are activated during bond breaking, which generally by itself contributes only a small fraction of the total energy loss (measured per unit fracture-surface area) [8–11]. Thus, the efficiency of the polymer's fracture toughness recovery (a macroscopic effect) is directly dependent on its efficiency to recover (heal) its broken DA cross-links.

The healing efficiencies of 3M4F and 2MEP4F polymers have been previously quantified using compact tension specimens with and without a crack-arresting central hole [6,7]. For 3M4F polymer, Chen et al. report healing at 150 °C with 50% efficiency and at 120 °C with 41% efficiency, although the sample fractured into two which precluded suitably accurate realignment of the fracture interfaces prior to healing [7]. These temperatures seem too high considering that dissociation of the DA bonds takes place to such an extent that at 150 °C the polymer essentially can be remolded into a new configuration. In the case of 2MEP4F polymer, a specimen with a crack-arresting hole was used and the fracture stopped at the hole [6]. The sample was then clamped and healed at 115 °C for 30 min. The pressure applied by this clamp was not quantified. Upon re-testing, the specimen fractured at an average of 78% of the original fracture load. At 115 °C, this polymer has an insignificantly small storage modulus, as shown in Fig. 2 and also in Fig. 4(b) of Chen et al. [6].

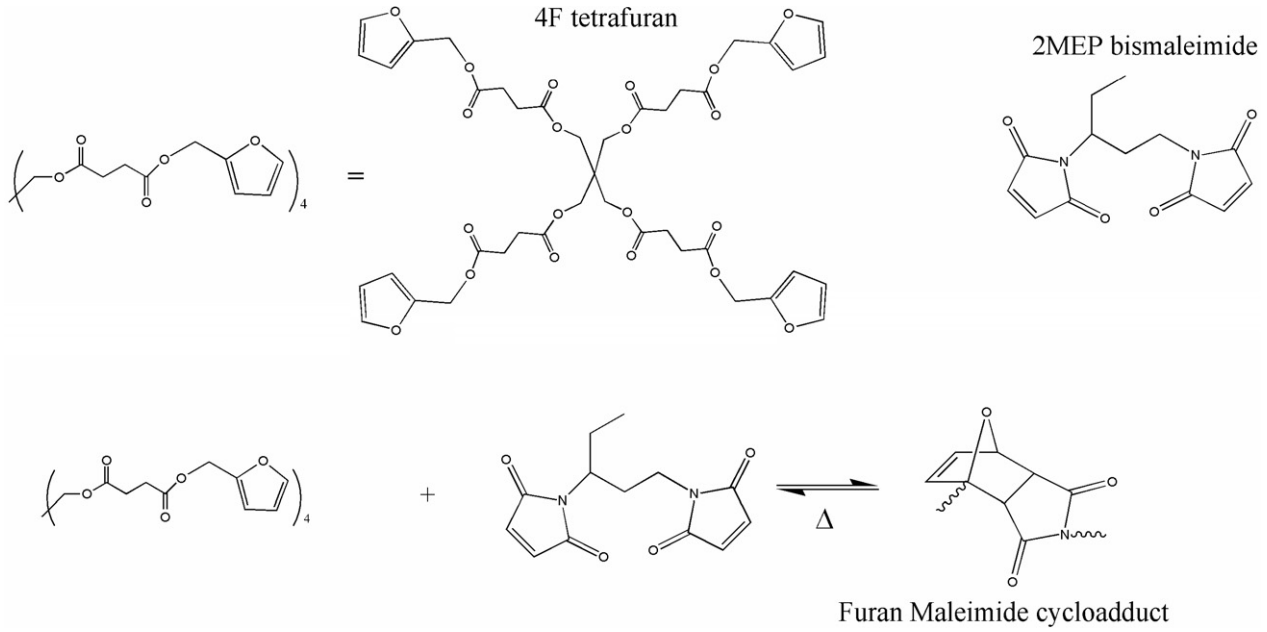

Fig. 1. The polymer consists of a multifuran molecule combined in stoichiometric ratio with a multimaleimide molecule to form 2MEP4F cycloadduct.

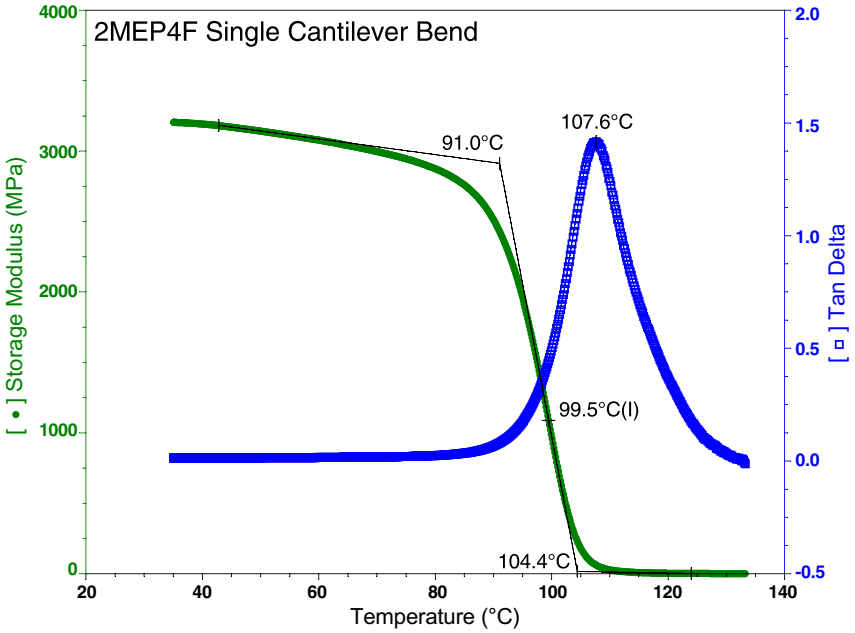

Fig. 2. Dynamic mechanical analysis of 2MEP4F polymer cycled at 1 Hz and heated at 3 °C min^{-1}.

We have thus sought to examine the repeated fracture–healing characteristics of the 2MEP4F polymer in a systematic and quantitative manner, using a sample geometry and relative dimensions that allow for controlled incremental crack growth while minimizing any potential inelastic deformation away from the crack tips. In the fracture mechanics literature, this sample is called the double cleavage drilled compression (DCDC) specimen, which is a relatively long column of rectangular cross section that contains a through-the-thickness central, circular hole with small notches at its axial crowns. Under an increasing uniform axial compression, cracks initiate at the crowns and grow axially in a stable manner, along the mid-plane of the sample; see Figs. 3 and 4. By careful displacement-controlled loading, the crack growth can be controlled to a certain extent. A unique property of this specimen geometry is that it renders the cracks self-arresting so that the fractured sample remains in one piece after the test, which greatly improves our ability to realign the fracture surfaces prior to healing. The sample may also be pre-cracked to a repeatable length to allow for a more accurate comparison between virgin and healed fracture loads, and, hence, fracture toughness. Moreover, multiple data points can be extracted from a single sample, making it well suited for quantifying the material's fracture toughness after several fracturing and healing cycles. To test the viability of this method, we verified the control of the fracture process using a number of samples made from poly(methylmethacrylate), arriving at remarkably consistent results [1]. In addition, based on these experiments, the relative dimensions (see Table 1) of the 2MEP4F samples were selected such as to allow for a direct measurement of the material's room temperature, quasi-static

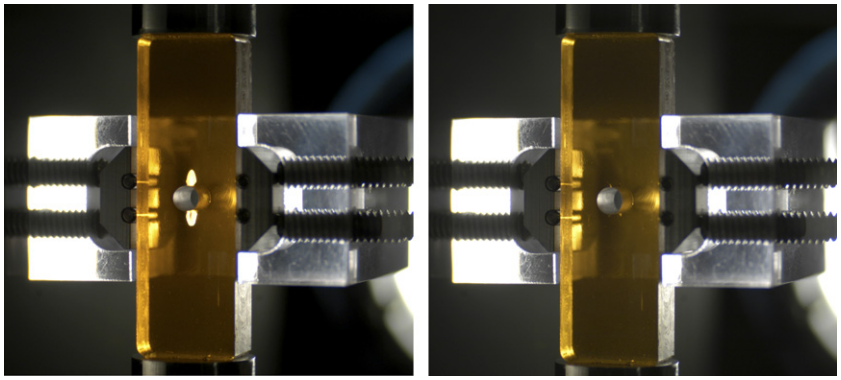

Fig. 3. Lateral confining fixture attached to specimen to create pre-crack. Left: specimen prior to axial compression with small razor notches visible at upper and lower crowns of central hole. Right: application of axial compression initiates cracks which propagate from razor notches and are arrested at a length of ~1.8 mm, which forms the pre-existing crack for subsequent fracture-toughness measurement.

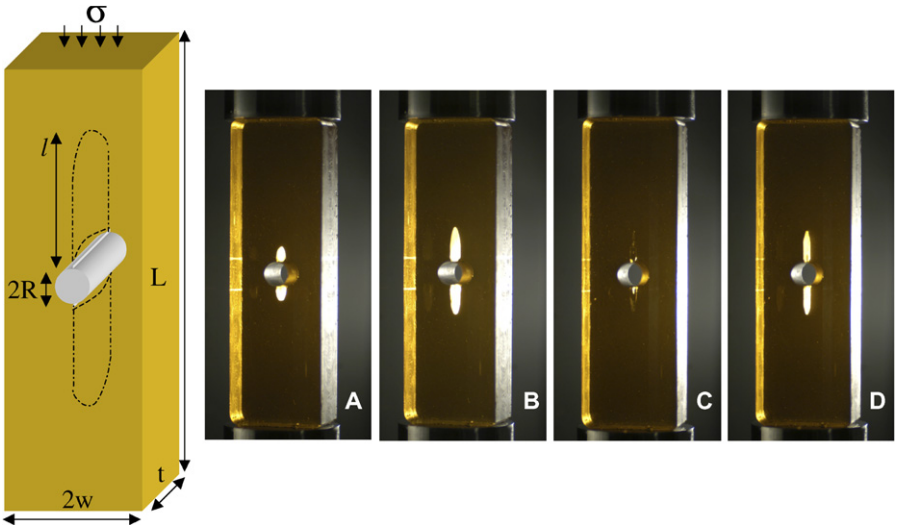

Fig. 4. Left: schematic of DCDC sample geometry. Dotted lines represent the location of the pre-crack and subsequent crack extension. Right: fracture and healing sequence of a single sample. (A) Virgin sample with hole and pre-cracks visible; (B) sample after first fracture event; (C) sample after first healing treatment; (D) sample after second fracture event.

fracture toughness without introducing unwanted inelastic deformations elsewhere within the specimen.

Our initial experiments on 2MEP4F samples were focused on the investigation of the healing efficiency reported previously by Chen et al. [6] for 2MEP4F polymer, attempting to duplicate the same treatment conditions as used in those experiments to induce healing, but using the DCDC sample geometry. To this end, a DCDC specimen of 2MEP4F polymer was fractured as previously described. The fractured sample was immediately placed inside an oven pre-heated to 115 °C, within a fixture that consisted of two flat surfaces lined with PTFE film, and loaded on the top surface such that a uniform pressure of 0.035 MPa was exerted normal to the crack interface. Two thermocouples were placed in close proximity to the sample to monitor the temperature of the sample and as a secondary measure of the oven's internal thermocouple. After 30 min the sample was cooled to room temperature over the course of 6 h. Upon removing from the fixture, it was evident that the sample had undergone significant creep, to the point that the 4 mm central hole was no longer visible. Although the crack had likewise disappeared, the sample could no longer be tested.

Table 1
Specimen dimensions

Specimen	Dimensions (mm)				
	l	*w*	*t*	*R*	*w*/*R*
1	50	7.8	8.8	1.98	3.95
2	50	7.8	8.3	1.98	3.95
3	50	7.8	8.2	1.98	3.95
4	50	7.8	9.3	1.98	3.95

The same experiment was repeated on another specimen; however, in this case no pressure was applied. The only load acting upon the sample was that of its own weight, oriented such that the crack interface was parallel to the surface on which the sample was resting. After the thermal treatment, as described above, the sample again had deformed due to creep. The resulting change in geometry made comparison between the virgin fracture event and successive fracture events impossible.

In this paper, we report the results of our repeated fracturing and healing cycles, where we have used the DCDC sample geometry and a more moderate thermal treatment for healing. We have observed that healing at reasonable temperatures, 85–95 °C, after repeated fracture–healing cycles, results in full fracture toughness recovery. We have then calculated the fracture toughness after each fracturing and healing cycle, using a model developed and tested in Plaisted et al. [1], arriving at reasonably consistent results for repeatedly healed 2MEP4F polymer.

2. Experiments

2.1. Sample fabrication

Bismaleimide (2MEP) and tetrafuran (4F) monomers were prepared according to procedures outlined in the literature [6,7]. Polymerization was carried out in the following way. Monomer 2MEP was heated above its melting point to a temperature of 95 °C. Furan monomer 4F was likewise heated to 95 °C to reduce its viscosity, and the two monomers were combined in stoichiometric proportion and mixed under vacuum for about thirty seconds. Prior to gelation, the pre-polymer was poured into molds constructed of silicone in the rectangular shape of the DCDC specimen geometry and held at 100 °C. A hard polymer

was formed within about 30 min at this temperature, though to ensure complete polymerization the samples were kept at this temperature for 15 h. The polymerized samples were then cooled to room temperature over a period of 10 h.

Four samples were machined to dimensions listed in Table 1 and labeled in Fig. 4. The w/R ratio, which influences the length over which the crack propagates in a stable manner, is about 4. We had already established that this relative dimension would also minimize possible inelastic deformations away from the crack tips [1]. The upper and lower surfaces of each specimen in contact with the loading platens were polished flat and parallel to within 0.013 mm.

2.2. Crack propagation

The method to pre-crack the sample involved wedging a blade into the central hole of the DCDC geometry, following the procedure reported previously, to create sharp notches at the axial crowns of the hole on the front and back surfaces of the specimen [1]. A restraining clamp was then placed around the sample and compression was applied in the axial direction. The clamp provided lateral confinement which prevented the cracks from growing beyond a length, l, of about 1.6 mm ($l/R \approx 0.8$) from the crowns of the hole. Fig. 3 illustrates the sample with confining clamp attached and the repeatable length to which the pre-cracks were propagated. Having introduced a uniform crack emanating from the upper and lower crowns of the hole, the clamp was removed and the specimen was then reloaded in compression to record the force and crack length of the subsequent fracture event.

Samples were loaded quasi-statically in an MTS Model 244.12 universal testing machine in displacement control with a 25 kN load cell. An external camera (Nikon D100) was focused at 4× magnification on the specimen. Each sample was compressed at a rate of 0.25 μm s^{-1}. The test was paused at increments of 25 μm in cross-head displacement and, after an equilibration period of about 10 s, the peak load over that period was recorded and a photograph was taken. The crack length in each photograph was later measured graphically by pixel counting software and correlated to the applied load. The crack length, l, was recorded as the average of the top and bottom crack lengths from each photograph, typically within a few per cent of one another, over the course of the experiment. The error within the load and crack length measurements was sufficiently low that error bars are not visible on the scale of the figures as presented. The healing treatment consisted of the following procedure. Following the fracture event, the sample was immediately placed inside a pre-heated oven at the desired temperature. The sample was placed within a pre-heated vise with two parallel surfaces lined with PTFE film such that a uniform pressure was applied normal to the crack interface. The vise was tightened to a uniform torque with each healing treatment, which correlated to applying roughly 0.35 MPa normal to the crack plane. Two thermocouples were placed in close proximity of the sample to monitor the temperature of the sample and as a secondary measure of the oven's internal thermocouple. The healing treatment was a two-stage process. The first stage consisted of heating the sample to 85 °C while applying pressure with the vise to bring the crack faces into intimate contact. After a period of time under this treatment, the crack was no longer visible. The vise was then removed and the sample was further heated to 95 °C for a period of time to maximize the mobility of the pendent furan and maleimide groups without inducing shape change (creep) in the sample.

The above healing procedure was derived from preliminary tests to determine the minimum treatment temperature at which the crack appeared to repair in a reasonable time period. At treatment temperatures below 80 °C with applied pressure of 0.35 MPa there was little to no change in the crack interface after 3 h. For treatment at 80–82 °C, the crack had partially disappeared. The areas towards the tips of the crack appeared to have been repaired, but the repair was less uniform towards the hole. When reloaded, the crack would re-open at a stress less than 10% of the stress required to extend the crack in the virgin specimen. For treatment in the range 83–85 °C, the healing was more uniform, though the stress required to re-open the crack was no more than 50% of the original stress. When this sample was heated to between 85 and 90 °C under pressure of 0.35 MPa, slight creep was observed. It was concluded that 85 °C was the maximum temperature at which the clamp pressure could be applied to the sample without inducing shape-changing creep.

In order to maximize the healing, a treatment method was proposed that would allow the crack interface to come back into intimate contact with applied pressure at the relatively low temperature, 85 °C. Once intimate contact and partial healing had been attained, the pressure could be removed and the temperature elevated (to 95 °C) to fully induce repair.

The picture sequence for the fracture and healing of a single specimen is shown in Fig. 4. After the first healing treatment, the crack largely disappears to the naked eye. When re-fractured, the crack appears to propagate along the same path as the original crack. This fracture–healing process is carried out multiple times on the same sample.

When the applied stress exceeds the critical fracture stress, or equivalently when K_I exceeds the K_{IC} of the material, the crack will grow. Because the sample geometry after healing is macroscopically identical to that before fracturing, the healing efficiency, η, may be calculated as a ratio of the stress required to propagate the crack to a given length in the healed material to the stress required to propagate the crack to approximately the same length in the virgin material. Since the fracture strength, as measured in terms of the stress-intensity factor, is proportional to the

corresponding critical stress, this would also measure the fracture strength after healing relative to that of the virgin sample, that is

$$\eta = \frac{\sigma_{\text{crit}}^{\text{healed}}}{\sigma_{\text{crit}}^{\text{virgin}}} \approx \frac{K_{\text{crit}}^{\text{healed}}}{K_{\text{crit}}^{\text{virgin}}}. \quad (1)$$

However, the efficiency defined in terms of the applied stress represents an actual measured quantity, whereas that in terms of the stress-intensity factor represents an estimate using a fracture model. The lack of control inherent in the fracture process precludes comparison of identical crack lengths and associated stresses in the virgin and healed fracture events. Rather, we can only compare critical stress values for cracks of roughly equivalent length. Healing efficiencies are listed in Tables 2–4 for each specimen and indicate how close the crack length in the healed and virgin cases was in terms of a positive (longer than the virgin crack) or negative (shorter than the virgin crack) percentage. Typically the length of the crack in the healed case was slightly shorter than the virgin crack, and as such provided a conservative estimate of healing efficiency. Since the crack propagates and arrests multiple times within one fracture cycle, the healing efficiency over that cycle may be averaged.

2.3. Specimen 1

During the first fracture event with this sample, the crack on each side of the hole jumped to a length (average of top and bottom lengths) of 1.6 mm from the crowns of the hole. As the load was increased the crack grew to 2.0 mm and then 2.3 mm. The load was removed and the sample was placed directly in a pre-heated vise within the oven set to 85 °C. Pressure was applied normal to the crack plane to a level of about 0.35 MPa. The sample remained at this temperature for 10 h. The clamping pressure was then removed and the temperature was elevated to 95 °C and held for a duration of 3 h, after which the sample was slowly cooled to room temperature.

The dimensions of the sample were measured to ensure that no change in shape had occurred due to the thermal treatment. The sample was then visually inspected under 4× magnification. A light was positioned behind the sample to reflect off the fracture plane. Typically the healed

Table 2
Healing efficiency of specimen 1

Crack length	$l/R = 0.84$			$l/R = 1.04$			$l/R = 1.10$			
	σ_{crit} (MPa)	η (%)	$\frac{l-l_{\text{virgin}}}{l_{\text{virgin}}}$ (%)	σ_{crit} (MPa)	η (%)	$\frac{l-l_{\text{virgin}}}{l_{\text{virgin}}}$ (%)	σ_{crit} (MPa)	η (%)	$\frac{l-l_{\text{virgin}}}{l_{\text{virgin}}}$ (%)	η_{avg} (%)
Virgin fracture	27.7	–	–	29.4	–	–	31.0	–	–	–
Healing 1	25.9	93	−7.3	29.4	100	2.3	30.8	100	−4.6	98
Healing 2	26.1	94	−5.2	29.4	100	2.3	30.8	100	−4.6	98
Healing 3	28.6	103	−1.2	30.3	103	−1.0	32.0	103	−0.2	103
Healing 4	29.2	106	5.9	31.7	108	2.4	32.5	105	−6.0	106
Healing 5	27.9	101	−6.9	31.3	106	−0.1	32.9	106	−2.4	104

Table 3
Efficiency of different healing procedures for specimen 2

Crack length	$l/R = 1.04$			$l/R = 1.15$			$l/R = 1.30$			
	σ_{crit} (MPa)	η (%)	$\frac{l-l_{\text{virgin}}}{l_{\text{virgin}}}$ (%)	σ_{crit} (MPa)	η (%)	$\frac{l-l_{\text{virgin}}}{l_{\text{virgin}}}$ (%)	σ_{crit} (MPa)	η (%)	$\frac{l-l_{\text{virgin}}}{l_{\text{virgin}}}$ (%)	η_{avg} (%)
Virgin fracture	29.0	–	–	29.2	–	–	30.5	–	–	–
Healing 1	28.4	98	−6.5	30.4	104	−2.1	32.2	105	−1.7	103
Healing 2	28.6	99	−1.1	29.5	101	−5.3	32.1	105	0.6	102
Healing 3	27.4	95	−15.9	29.2	100	0.2	30.8	101	−4.3	98
Healing 4	26.0	90	−10.5	28.0	96	1.4	29.8	98	1.9	95

Table 4
Healing efficiency of specimen 3

Crack length	$l/R = 1.33$			$l/R = 1.62$			$l/R = 1.96$			
	σ_{crit} (MPa)	η (%)	$\frac{l-l_{\text{virgin}}}{l_{\text{virgin}}}$ (%)	σ_{crit} (MPa)	η (%)	$\frac{l-l_{\text{virgin}}}{l_{\text{virgin}}}$ (%)	σ_{crit} (MPa)	η (%)	$\frac{l-l_{\text{virgin}}}{l_{\text{virgin}}}$ (%)	η_{avg} (%)
Virgin fracture	28.2	–	–	29.0	–	–	30.7	–	–	–
Healing 1	26.4	94	−2.2	28.1	97	3.9	29.6	96	−8.6	96
Healing 2	29.0	103	−13.7	32.1	111	−0.8	33.8	110	−8.6	108
Healing 3	29.2	104	−13.2	32.4	112	−5.8	34.5	112	−3.6	109
Healing 4	31.1	110	−14.5	34.0	117	0.0	35.4	115	−4.4	114

specimen would bear minor evidence of the previous crack plane in the form of scar-like striations. It was further noted that the initial pre-cracks created by the blade were clearly evident after the healing process. The light reflecting from the pre-cracks was significantly more intense than the light reflecting off the healed interface, indicating that the material on either side of the pre-cracks was still distinctly separated. A typical picture sequence for the fracture and healing process is given in Fig. 4. After making these observations, the sample was then loaded in an identical manner to that used for fracturing of the sample in its virgin state.

During reloading of the healed sample, it was noted that the crack grew in a more stable manner compared with crack propagation in the virgin case. As a result, the crack grew in smaller increments and at lower velocity, thus yielding a greater number of data points per unit crack length. This was likely due to the fact that the material had previously cracked along the same plane. The fracture proceeded with a similar load vs. crack length data to the virgin fracture to suggest nearly complete healing.

The sample was fractured, healed and re-fractured for five consecutive cycles, using the above-outlined procedure. During the second and third fracturing cycles (following the first and second healing cycles, respectively), the load was removed when the crack had propagated to approximately the same length as that obtained in the virgin state. On the fourth fracturing cycle, the crack was propagated beyond the original length and into previously uncracked material. As such, this extension of the crack can be considered occurring within virgin material. In fracture cycle 5 (after healing cycle 4), the crack was extended to approximately the same length as in fracture cycle 4. In fracture cycle 6, the loading was continued until the crack had propagated to within a few millimeters of the ends of the sample, which may have introduced inelastic deformation of the specimen at its ends and at the horizontal crowns of the hole. The same healing treatment was performed and it was noted that the crack had disappeared over just a portion of the entire interface, further suggesting the effect of the permanent deformations mentioned above. Due to this, during fracture cycle 7, very little load was required to propagate the partially healed crack back to its full length, indicating that minimal healing had actually occurred. Thus, because of the inelastic deformation during the preceding severe fracturing, the cracked surfaces did not come back into complete contact under the pressure that was applied. Also, since the crack had grown to the far ends of the sample, it was likely that the crack faces did not match up again since there is more surface topology to "key" back together. The results of these fracture–healing cycles are presented in Figs. 5 and 6, as applied axial compressive stress vs. crack length, excluding the results obtained for the damaged sample in the last cycle. The length refers to the average of the top and bottom crack lengths, l, normalized with respect to the radius of the central hole, R. Each set of data points is identified by its state prior to each fracturing process; e.g. "Healing 2" refers to fracturing data after the specimen had been healed for the second time.

Table 2 lists the healing efficiencies for specimen 1 and indicates how close the crack length in the healed and virgin cases was in terms of a positive (longer than the virgin crack) or negative (shorter than the virgin crack)

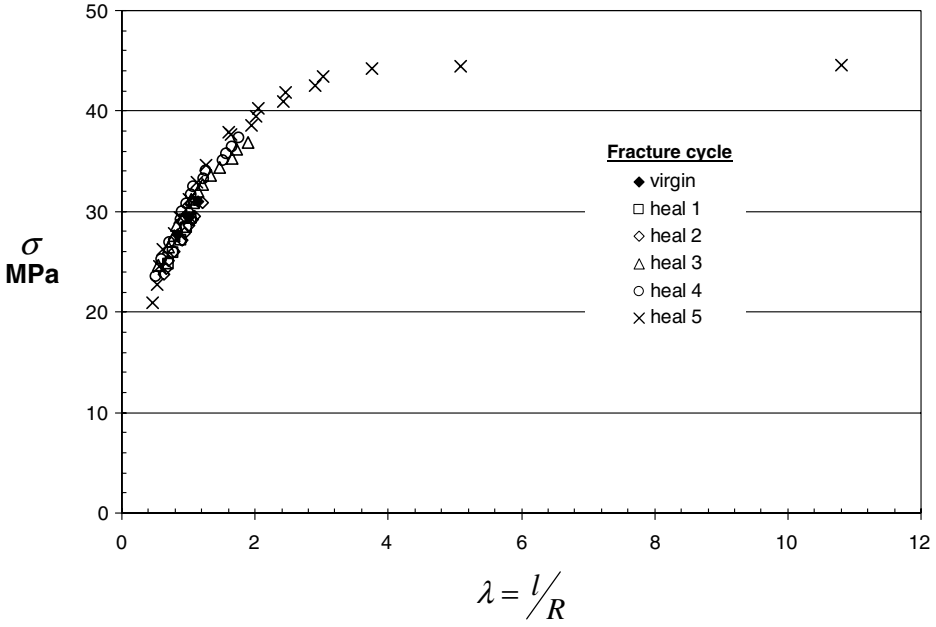

Fig. 5. Stress vs. crack length data of five fracture–healing cycles for specimen 1. All healing treatments for specimen 1 consisted of applying pressure while heating to 85 °C for 10 h followed by heating to 95 °C for 3 h with no applied pressure.

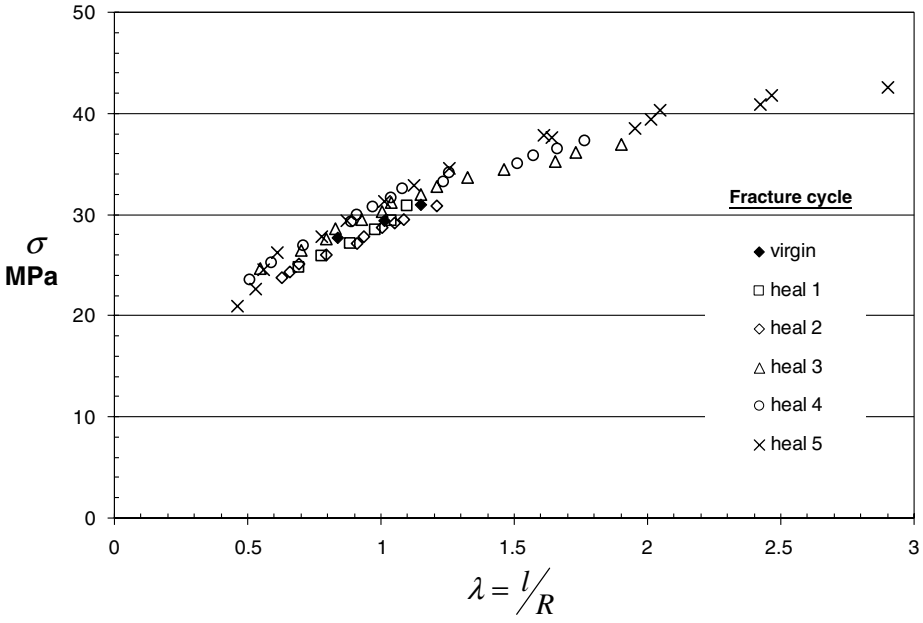

Fig. 6. Initial portion of stress vs. crack length data shown in Fig. 5 for specimen 1.

percentage. The table also includes the average healing efficiency for each healing cycle, η_{avg}. This is calculated by averaging the values of the healing efficiency obtained at various crack lengths over the corresponding fracture cycle.

2.4. Specimen 2

Specimen 1 demonstrated the ability of the 2MEP4F polymer to heal at various lengths along the crack path, over five cycles of cracking and healing. In specimen 2, similar measurements were performed, but the duration of the heat treatment was reduced. It was observed in specimen 1 that the crack would essentially disappear when the sample had reached thermal equilibrium in the oven at about 85 °C, which would occur within about 5 min; further discussion on this observation is detailed below. The sample was kept at this temperature for 10 h (overnight) both as a precaution and for experimental convenience. For specimen 2, the first healing treatment followed the same routine as for specimen 1 to substantiate those results, where the sample was held at 85 °C for 10 h under pressure, followed by 3 h at 95 °C without pressure. For healing treatments 2 and 3 the thermal treatment time was reduced to holding at 85 °C for 1 h with pressure, followed by 1 h at 95 °C without pressure. Reducing the treatment time by this amount seemed to have no effect on the healing efficiency of specimen 2. For healing treatment 4, the thermal treatment time was further reduced to holding at 85 °C for 30 min with pressure, followed by 30 min at 95 °C without pressure. Again, this treatment showed little effect on the healing efficiency of specimen 2. In healing treatment 5, specimen 2 was held at 85 °C for 30 min with pressure and visually the degree of repair was similar to previous treatments at the same time and temperature. The additional treatment at 95 °C was not carried out in treatment 5. The crack initiated at a relatively low load and then extended to a length comparable to the crack in the previous fracture cycle, indicating very low healing efficiency. Upon further loading the crack extended to near the full length of the sample at a stress well below what was expected by the previous trends. This test indicated the importance of the secondary treatment at 95 °C. All results for this sample are given in Figs. 7, 8 and Table 3.

2.5. Specimen 3

Specimen 3 was used to substantiate the results obtained from specimen 2, namely continuing the healing treatment at 85 °C for 30 min under pressure, followed by 95 °C for 30 min without pressure. Again, this healing treatment showed near complete repair over four fracture–healing cycles. During the fourth loading, the crack was extended to near the full length of the sample. The sample was healed and re-fractured, showing essentially complete recovery of the previous fracture characteristics over the entire crack length. Results for specimen 3 are given in Figs. 9, 10 and Table 4.

2.6. Specimen 4

To estimate the fracture toughness of the virgin material, a single specimen was subjected to complete fracture to establish the characteristic stress vs. normalized crack length. No healing was carried out on this specimen. The results were then used in conjunction with the

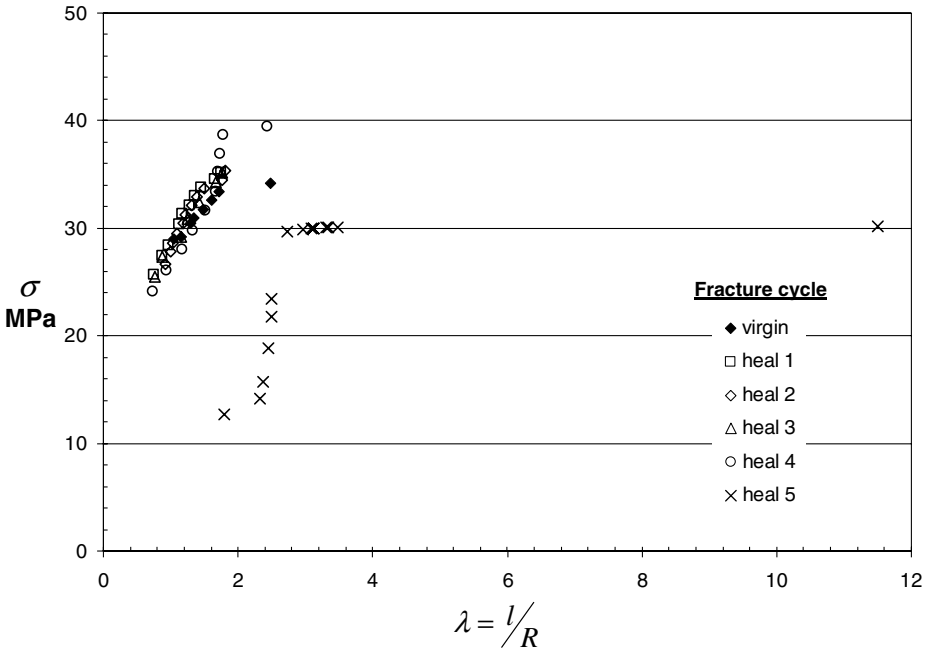

Fig. 7. Effect of different healing treatments on the resulting fracture strength of specimen 2.

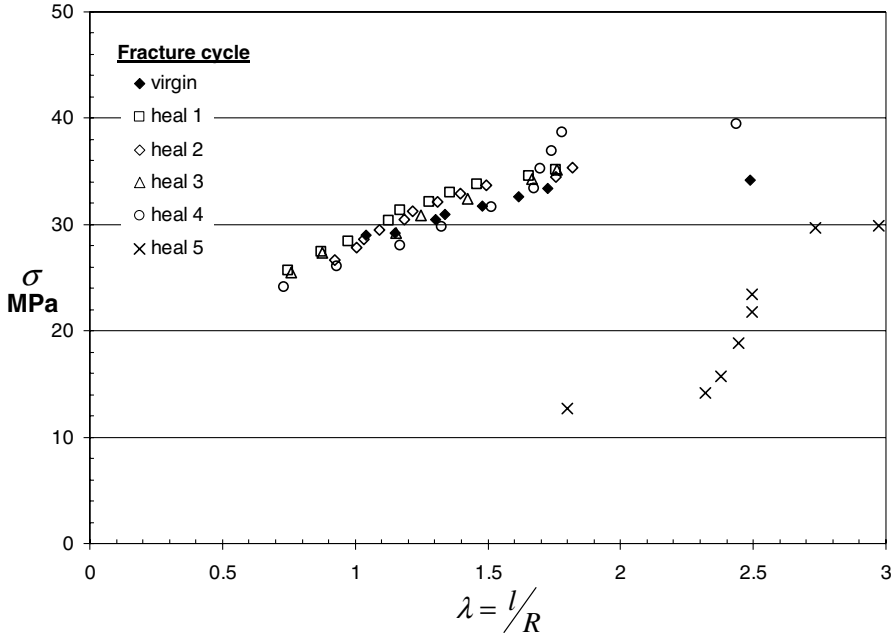

Fig. 8. Initial portion of stress vs. crack length data shown in Fig. 7 for specimen 2.

model that had already been developed for long and short cracks in a DCDC sample [1]. The final results of this model are outlined below and compared with the data of specimen 4.

2.7. Correlation to the model

To model the crack growth phenomenon in a DCDC sample, Plaisted et al. [1] consider first a pair of short cracks emanating from the crowns of the central hole and growing axially under a monotonically increasing axial compression, and seek to estimate the resulting stress-intensity factor. To this end, they represent the tensile stress field, created by an axial, uniform compression in an infinite plate normal to the axial plane that passes through the center of the hole, by an equivalent pair of concentrated forces of magnitude P, acting at the distance x from the center of the hole, where

$$P = Rd\sigma_0(l), \quad x = eR. \tag{2,3}$$

Here, $\sigma_0(l)$ is the axial compression, l is the crack length, and $d = 1/\sqrt{27}$ and $e = 3\sqrt{3}(2 - \ln 3)/4$ for an infinite plate. The resulting stress-intensity factor can now be readily calculated, leading to the following expression:

$$\frac{\sigma_0(l)\sqrt{w}}{K_c} = \frac{\sqrt{w/R}\sqrt{\pi(1+\lambda)}}{d\left(\sqrt{\frac{1+\lambda+e}{1+\lambda-e}} + \sqrt{\frac{1+\lambda-e}{1+\lambda+e}}\right)}, \tag{4}$$

where w, the half-width of the sample, and K_c, the critical stress-intensity factor, are used to make the equation dimensionless, and $\lambda = l/R$. To account for the fact that the sample width, w, is finite, we now let d be a function of l/R and based on data reported by Plaisted et al. [1], set

$$\frac{d(w/R)}{d_\infty} = 5.7 - 0.75\frac{w}{R}, \tag{5}$$

where $d_\infty = 1/\sqrt{27}$. We note that the linear approximation (4) has a limited range of applicability, but should be sufficient for our current geometry. Expression (3), with approximation (4), is valid while the crack is relatively

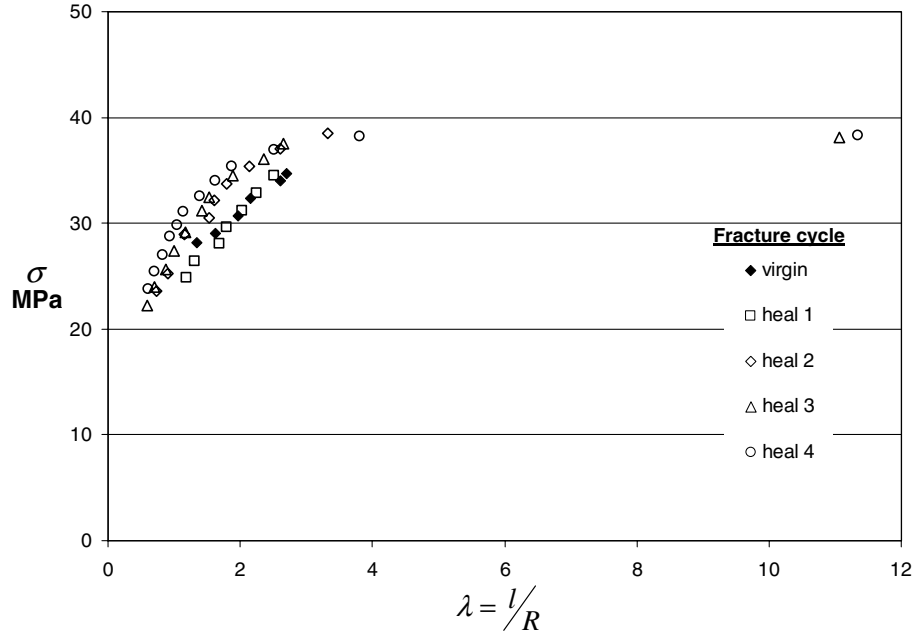

Fig. 9. Fracture and healing on specimen 3.

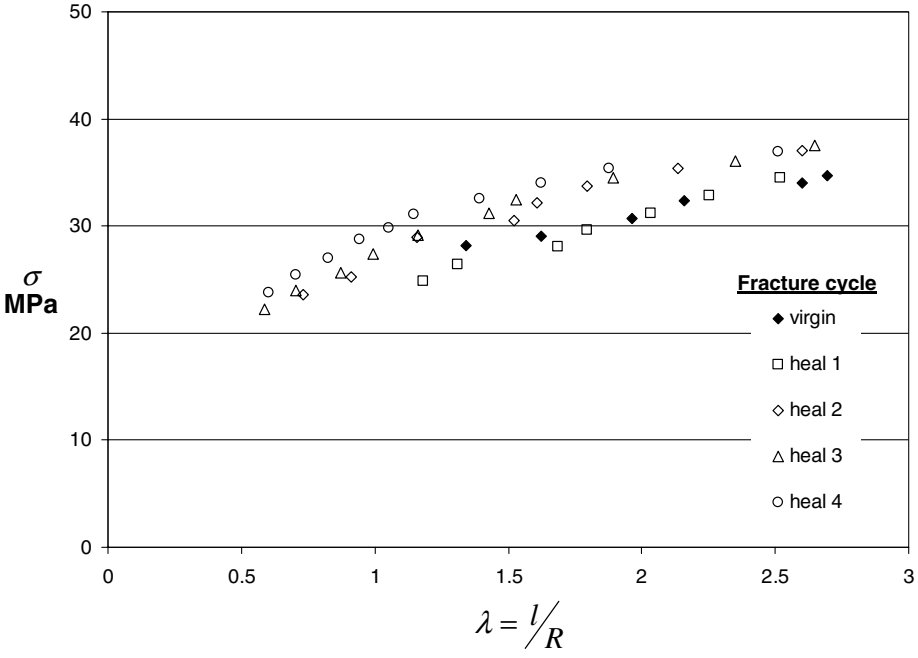

Fig. 10. Initial portion of stress vs. crack length data shown in Fig. 9 for specimen 3.

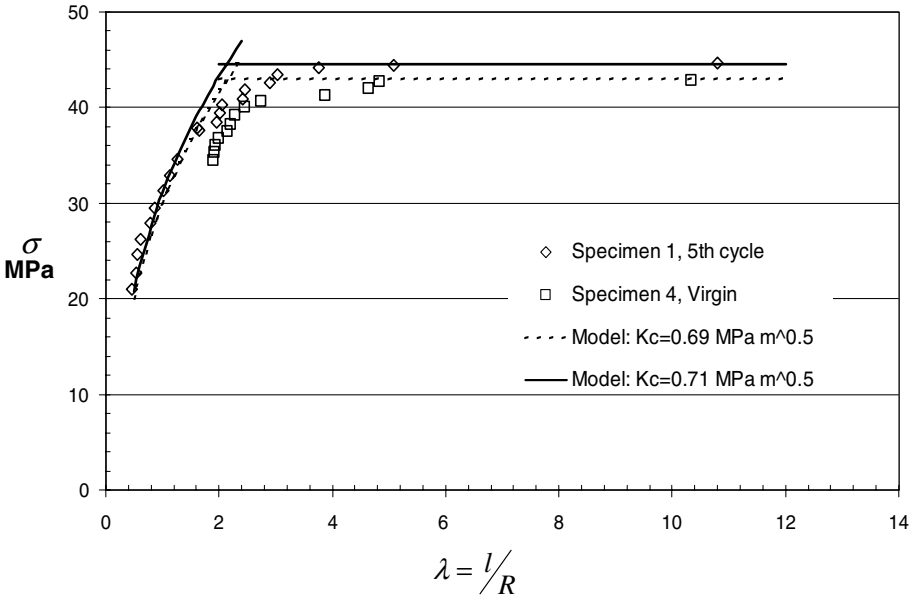

Fig. 11. Fracture into virgin polymer for specimen 4 in relation to model prediction with $K_c = 0.692$ MPa $m^{1/2}$, and specimen 4 after five cycles of fracturing and healing with $K_c = 0.716$ MPa $m^{1/2}$.

short. For the long-crack approximation, we consider a beam-column model and, as detailed in Plaisted et al. [1], arrive at the following expression for the axial stress vs. crack length:

$$\frac{\sigma_0\sqrt{w}}{K_c} = \frac{w/R}{2g(w/R)}, \tag{6}$$

where the function $g(w/R)$ is given by

$$g(w/R) = \frac{3 + 2\ln(w/R)}{4(w/R)} - \frac{1}{4(w/R)^3}. \tag{7}$$

Eq. (5) suggests that the axial stress remains constant once the crack is suitably long. A more complete estimate shows that the axial stress should increase slightly as the crack length increases.

To estimate the material's K_c, we use Eqs. (5) and (6), together with the plateau value of the axial stress. We then use this value of K_c in Eq. (3) to model the short crack growth regime. From Fig. 11, the plateau value of the axial stress is about 43 MPa, which yields a value of about 0.69 MPa $m^{1/2}$ for the fracture toughness. With this value, the solid curves in Fig. 11 are obtained. As an additional comparison, we have also included in this figure the results obtained after the fifth cycle of fracturing and healing for specimen 1, which suggest some increase in the fracture toughness due to repeated healing. In this case, the plateau value is 44.3 MPa, with a fracture toughness of 0.72 MPa $m^{1/2}$.

3. Discussion

Our experiments demonstrated the healing efficiency of the 2MEP4F polymer to be near complete over several cycles of fracturing and healing, using a healing process at moderate temperatures and pressures so that no dimensional changes are introduced due to creep. In addition, we have used a sample geometry that allows for quantitative evaluation of the fracture toughness of the virgin and healed polymer. We have also experimentally examined the effect of different healing treatments on the fracture strength of the healed polymer, using various healing periods and temperatures. The results clearly demonstrate the repeated healability of this class of polymers. They are in contrast to the previous fracture–healing studies of this class of polymers that have used high temperatures at which the polymer loses its stiffness and in fact can be molded into different geometries [6,7]. Notwithstanding the high temperature treatments, Chen et al. [6] obtain for 2MEP4F polymer a healing efficiency of 78% for a treatment at 115 °C and an efficiency of 41% at 120 °C, and 50% at 150 °C for 3M4F polymer, at which temperatures both polymers would undergo extensive creep under small pressures. Indeed, healing at these temperatures results from the repair of both the fractured bonds and the thermally liberated bonds, whereas at temperatures that we have used, healing only occurs between fractured bonds. Multiple healing events are shown to be possible along the same fracture path and are most repeatable when the crack length is kept below the plateau value of the axial stress as described in our model, to avoid excessive bending that would produce inelastic deformation in the sample.

In this work, we have noted that at 85 °C visual healing will take place within 30 min, though it may be incomplete. Further heating to 95 °C, a temperature around the onset of the glass transition, provides additional energy for the remaining unreacted moieties to re-combine. At this temperature, the applied pressure is removed to avoid creep within the specimen since the stiffness of the material is

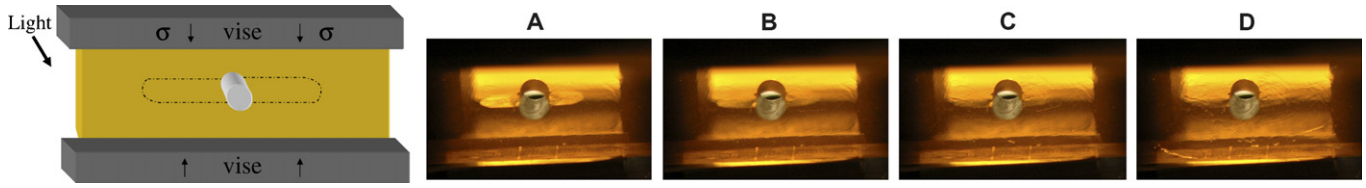

Fig. 12. Illustration of in-situ photos of representative healing treatment at 85 °C. Left: orientation of sample with respect to camera. Right: sequence of photos during treatment at 85 °C. (A) Time 0; (B) 2 min; (C) 4 min; (D) 15 min.

reduced. In theory, the bond will self-repair at temperatures below 110 °C provided that the broken moieties come into contact. Heating provides sufficient conformational motion in the polymer structure to bring the de-bonded maleimide and furan groups into close proximity. Chen et al. have shown that polymerization between similar furan and maleimide moieties at room temperature requires many days and reaches only 60–70% cross-linking [7,12].

The data suggest that the degree of healing does not increase with increasing the treatment time beyond 1 h. Similar healing efficiencies were obtained for the 10 h (85 °C) followed by 3 h (95 °C) treatment as for the 0.5 h (85 °C) followed by 0.5 h (95 °C) treatment. Fig. 12 illustrates in situ photos of progressive stages of healing during the thermal treatment of specimen 3. These photos provide an estimate of when the crack undergoes most of its (visual) repair. At about 4 min after being placed in the oven at 85 °C, the crack essentially disappears. Calculations based on the heat capacity (1.3 J g^{-1} $°C^{-1}$) and an estimated thermal conductivity (0.25 W m^{-1} $°C^{-1}$ average for polyimides) indicate that it should take about 3 min for the center of the sample to reach 85 °C. During initial polymerization of these monomers at 95 °C, we have noted that the mixture begins to gel within about 3 min after combination. Likewise the re-polymerization of bonds across the cracked interface is also rapid at these temperatures.

That the degree of healing does not improve with time beyond that required to reach thermal equilibrium is in contrast to the healing observed in the welding of thermoplastic polymers [13–15]. The recovery of strength in welded thermoplastics shows a time dependence that corresponds to the diffusion of polymer chains across the interface. Healing in the 2MEP4F polymer occurs rapidly at 85 °C, after the sample has reached thermal equilibrium, which indicates it is not a diffusion-controlled process; rather it occurs on a timescale controlled by the kinetics of the Diels–Alder reaction to re-connect the broken cross-linking bonds that then leads to the recovery of the overall macroscopic fracture toughness.

The data suggest that the samples became slightly more resistant to fracture with successive healing treatments, a trend that was observed consistently for all three samples. One may suspect that the increased thermal treatment exposes the sample to heat for longer periods, rendering it stronger perhaps due to an increase in the degree of conversion in the polymerization. This, however, is not supported by the fact that shorter thermal treatments resulted in the same full recovery as the longer treatments. Also, samples were cured for 15 h at 100 °C to maximize the degree of conversion during polymerization. Thermal analysis by differential scanning calorimetry had indicated no further change in the polymer after this treatment.

Another possible cause may be due to the difference in velocity of crack propagation in the virgin and healed cases. In the virgin material, the sample would incrementally build-up elastic energy with increasing applied load, and upon reaching a critical stress the crack would rapidly propagate some distance before arresting. Then this process would be repeated for the next incremental crack growth. Fracture through the healed interface proceeded in a more gradual manner, as indicated by the greater number of data points per length of crack propagation in the healed samples. There was less build-up of elastic energy before the crack would propagate. As such, the crack would propagate at a lower velocity and could be arrested after traveling a smaller distance, which would appear in the data as bearing a greater stress for a given crack length. This suggestion would imply imperfect healing along the crack plane, though in the data it would give the appearance that the sample had healed to a greater degree than the original material.

Acknowledgements

The authors wish to thank Fred Wudl and Xiangxu Chen for sharing their expertise in synthesizing the bismaleimide and tetrafuran monomers used in this work. Jon Isaacs and Benjamin Cook are also acknowledged for their many helpful discussions on the mechanical testing of these polymers. This work has been supported by DARPA (Dr. Leo Christodoulou's Synthetic Multifunctional Materials Program) through ARO DAAD19-00-1-0525 contract to the University of California, San Diego.

References

[1] Plaisted TA, Amirkhizi AV, Nemat-Nasser S. Compression-induced axial crack propagation in DCDC polymer samples: experiments and modeling. Int J Fract 2006;141:447.
[2] White SR, Sottos NR, Guebelle PH, Moore JS, Kessler MR, Sriram SR, et al. Autonomic healing of polymer composites. Nature 2001;409:794.
[3] Engle LP, Wagener KB. A review of thermally controlled covalent bond formation in polymer chemistry. J Macromol Sci 1993;C33:239.

[4] Imai Y, Itoh H, Naka K, Chujo Y. Thermally reversible IPN organic–inorganic polymer hybrids utilizing the Diels–Alder reaction. Macromolecules 2000;33:4343.
[5] Chujo Y, Sada K, Saegusa T. Reversible gelation of polyoxazoline by means of Diels–Alder reaction. Macromolecules 1990;23:2636.
[6] Chen X, Wudl F, Mal A, Hongbin S, Nutt SR. New thermally remendable highly cross-linked polymeric materials. Macromolecules 2003;36:1802.
[7] Chen X, Dam MA, Ono K, Mal A, Hongbin S, Nutt SR, et al. A thermally re-mendable cross-linked polymeric material. Science 2002;295:1698.
[8] Robertson RE, Sporer MG, Pan T-Y, Mindroiu VE. Plasticity of brittle epoxy resins during debonding failures. J Mater Sci 1989;24:4106.
[9] King NE, Andrews EH. Fracture energy of epoxy resins above T_g. J Mater Sci 1978;13:1291.
[10] Kinloch AJ, Young RJ. Fracture behavior of polymers. London: Applied Science Publications; 1983.
[11] Andrews EH, Stevenson A. Fracture energy of epoxy resin under plane strain conditions. J Mater Sci 1978;13:1680.
[12] Chen X. Novel polymers with thermally controlled covalent cross-linking. Chemistry. Los Angeles: University of California Los Angeles; 2003. p. 159.
[13] Wool RP, O'Connor KM. Time dependence of crack healing. J Polym Sci: Polym Lett Ed 1982;20:7.
[14] Wool RP. Polymer interfaces: structure and strength. Hanser; 1995.
[15] Kausch HH, Tirrell M. Polymer interdiffusion. Ann Rev Mater Sci 1989;19:341.